Water Splitting on Ti-Oxide-Terminated SrTiO 3 (001)

Vladyslav Solokha, Debi Garai, Axel Wilson, David Duncan, Pardeep Thakur, Kurt Hingerl, Jörg Zegenhagen

THE JOURNAL OF PHYSICAL CHEMISTRY C

Article

Cite This: J. Phys. Chem. C XXXX, XXX, XXX−XXX

pubs.acs.org/JPCC

Water Splitting on Ti-Oxide-Terminated $SrTiO_3(001)$

Vladyslav Solokha,[†,‡] Debi Garai,[†,§] Axel Wilson,[†] David A. Duncan,[†] Pardeep K. Thakur,[†] Kurt Hingerl,[‡] and Jörg Zegenhagen*[,†]

[†]Diamond Light Source Ltd, Harwell Science and Innovation Campus, Didcot OX11 0DE, U.K.

[‡]Johannes Kepler Universität Linz, Altenberger Straße 69, A-4040 Linz, Austria

[§]Amity University, Noida Campus, Noida, UP 201303, India

Supporting Information

ABSTRACT: Combining X-ray photoelectron spectroscopy with the standing wave technique, we investigated adsorption of a monolayer of water on Ti-oxide-terminated $SrTiO_3(001)$ in ultra-high vacuum (UHV). At room temperature, the surface is water-free but hydroxylated. A quarter monolayer of hydroxyl is tightly bound 1.85 ± 0.06 Å above the TiO_2 surface. Deposited at a low temperature, a monolayer of water adsorbs with the oxygen located 2.55 ± 0.2 Å above the surface, apparently close to atop Ti, but H_2O is unstable at 200 K. A fraction desorbs, in part under the X-ray beam, but a major fraction of H_2O dissociates immediately, with the liberated hydrogen most likely attaching to a surface oxygen. The produced hydroxyls bind only loosely to the surface, are unstable at 200 K, and rapidly desorb once the surface is water-free. Although our study was conducted in UHV, the presented results suggest that Ti-oxide-terminated $SrTiO_3(001)$ may possess a high catalytic activity toward hydrolysis under realistic conditions.

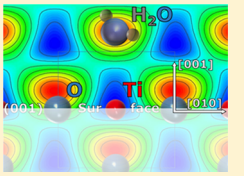

INTRODUCTION

The goal of identifying materials, routes, and strategies for carbon-neutral renewable energy production such as directly producing hydrogen fuel, eventually on an industrial scale, motivates intensive research. A promising path toward fuel production from water and sunlight involves photo-electrochemistry, suggested by the early finding of Fujishima and Honda[1] of electrochemical photolysis of water at a TiO_2 electrode. Soon afterward, the photocatalytic activity of $SrTiO_3$ (STO) in the water splitting reaction was also reported.[2,3] In the present study, we deposited a monolayer (ML) of water on STO(001) at a low temperature in ultra-high vacuum (UHV) on an atomically clean, titanium-oxide-terminated surface that was partially reconstructed. We find that the majority of the water layer in contact with the Ti-oxide-terminated surface deprotonates rapidly. This demonstrates that the (001) surface of STO exhibits a very low activation barrier toward decomposition of water. Although our study was conducted under UHV conditions and we could not analyze the reaction products, the study suggests that STO(001) possesses a high catalytic activity in the water splitting reaction.

The cubic (a = 3.905 Å) perovskite STO (see Figure 1a) is a semiconductor with a wide, 3.1 eV band gap that is stable in electrolytes under alkaline conditions.[4] Just as TiO_2, STO is nontoxic and fairly inexpensive (O, Ti, and Sr rank 1, 9, and 16 in earth's crust abundancy), which are favorable pre-conditions for a catalyst of wide use. As a ternary transition metal oxide, STO offers a rich playground for material engineering (see, e.g., refs 5−8) that may open up new ways of employing the material in energy applications. STO becomes n-type conducting (and superconducting[9]) via doping, e.g., by oxygen vacancies or Nb^{5+} substituting for Ti^{4+}. The (001) surface of

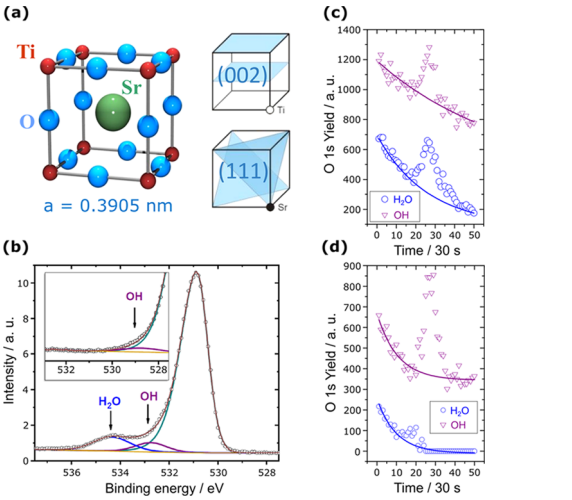

Figure 1. (a) Unit cell of the cubic perovskite $SrTiO_3$. The (002) and (111) diffraction planes are indicated on the right-hand side with spacings d_{002} = 1.95 Å and d_{111} = 2.25 Å, respectively. The (002) diffraction planes are the alternating TiO_2 and SrO planes. (b) X-ray photoelectron spectrum (3.165 keV) of O 1s after H_2O deposition. The inset shows the OH component at room temperature. (c, d) XSW scans, $\Delta E \approx 10$ eV around the $SrTiO_3$ (111) (c) and (002) (d) reflections at 2.76 and 3.18 keV, respectively, on two different parts of the water-dosed surface, plotted as a function of measuring time.

STO has two possible terminations, either TiO_2 or SrO, but annealing in UHV leads to Sr depletion and Ti-oxide-rich

Received: February 22, 2019
Revised: May 31, 2019
Published: June 25, 2019

surfaces. Depending on preparation conditions, several reconstructions such as (2 × 1), (2 × 2), $c(2 \times 4)$, and $c(2 \times 6)$ are observed (see, e.g., refs 10, 11).

The interaction of water with STO, focusing largely on the (001) surface, has been explored experimentally[12−25] and by total energy calculations.[22,23,26−31] Most computational studies concentrated on the 1 × 1 SrO and/or TiO_2 bulk terminated, unreconstructed substrate with only a few exceptions considering reconstructed surfaces.[29−31] The vast majority of the experimental studies used spectroscopy techniques, in particular, photoelectron spectroscopy (PES), whereas Hussain et al.[24] employed surface X-ray diffraction (SXRD), investigating the structure of liquid water in contact with the STO(001) surface in situ, at ambient temperature. They concluded, as have most other studies, that water adsorbs preferentially intact on the Ti-oxide-terminated STO(001) surface, showing little tendency toward deprotonation. Yet, in support of the dissociative adsorption of water on the TiO_2-terminated surface of STO(001) are the results of the more recent density functional theory studies by Guhl et al.[27] and Holmström et al.[31] The latter concluded that 10−15% of oxygen are hydroxylated on the TiO_2-terminated surface at all water coverages, and the former concluded that at least at lower coverages the TiO_2-terminated surface decomposes water with the molecular state being stable at higher coverages. Beccera-Toledo et al.[23,29] even concluded that hydroxyls are essential for the formation of some of the Ti-oxide-rich STO(001) reconstructions.

To investigate this issue further, we combine here the chemical sensitivity of PES with the X-ray standing wave (XSW) technique[32] to study the deposition and reaction of a monolayer of water on Ti-oxide-terminated STO(001) at low temperature. With the help of PES, we distinguish OH and H_2O by their O 1s electron binding energy, and XSW analysis provides additional information about their surface location.[33] Our study reveals that more than 50% of H_2O deprotonates rapidly and the remainder desorbs at ∼200 K. The produced hydroxyls are loosely bound, thus volatile, and desorb rapidly from the water-free surface. This finding indicates that Ti-oxide-terminated $SrTiO_3$(001) may be more effective in the hydrolysis of water than commonly believed.

A 1/4 ML of OH remains on the surface after desorption of water. It is stable at room temperature at a position 1.85 ± 0.06 Å above the surface, most likely (close to) atop Ti, which would be in agreement with DFT calculations.[26−28] It is present on the Ti-oxide-terminated surface even without water exposure and may be involved in the reconstructions of the Ti-oxide-terminated surface. The O 1s signal of the volatile hydroxyls shows the same binding energy as that of the tightly bound OH, which is astonishing given their obviously significantly different surface binding energy, but with the help of the XSW structural data we could distinguish both.

EXPERIMENTAL SECTION

The XSW/PES experiments were carried out at beamline I09[34] at the Diamond Light Source, using STO(002) and (111) Bragg reflections close to 90°, around excitation energies E_γ = 3.18 keV and E_γ = 2.76 keV, respectively. We used unfocused X-rays with a size of 300 × 300 μm^2 to minimize beam effects. For the photoelectron analysis, we used a Scienta EW 4000 HAXPES hemispherical energy analyzer equipped with a MCP/CCD detector. The wide-angle lens has its center pointing in the direction of the horizontally polarized X-ray beam, with a horizontal acceptance of ±30°. For the (002) XSW measurements, photoelectrons were detected at grazing emission angle (i.e., 0 to 30°) with the STO(001) surface and at an emission angle of ∼60° (±30°) for the (111) XSW measurements. A niobium (0.1%)-doped, 5 × 10 mm^2 STO sample with (001) orientation (Crystal GmbH Berlin) was cleaned by Ar sputtering and annealed at a moderate temperature to produce a Ti-oxide-terminated surface that low-energy electron diffraction revealed being in part reconstructed (see the Supporting Information for more details).

In a preparation chamber, separated from the analysis chamber by a gate valve but sharing the manipulator to allow transfer without loss of cooling, we exposed the atomically clean STO(001) surface at T < 200 K to 2 × 10^{-8} mbar H_2O for 30 s, i.e., to 0.6 Langmuir, which lead to the adsorption of about one monolayer of water. In accordance with other works (e.g., ref 28), we define a monolayer as a dense packed layer of H_2O with a thickness of 2 Å, containing two H_2O (or OH) molecules per STO(001) surface unit cell. Since water desorbs in several stages from the STO(001) surface already below room temperature, with the last monolayer commencing to desorb above 200 K,[19] we kept the sample at 200 K during the XSW/PES measurements. We determined absolute coverages by referencing the OH and H_2O signals to the STO bulk oxygen O 1s yield, taking into account the electron escape angle, the effective attenuation length of the O 1s electrons in the STO, and the electron attenuation of the O 1s bulk electrons in the overlayer. While all determined coverage values are accurate to ±20% relative to each other, the error in absolute values may be as large as ±40% (more details are available in the Supporting Information).

Differing from diffraction techniques, XSW measurements are phase-sensitive and allow direct determination of atomic distances. The technique has been reviewed extensively, and we repeat here only its basics. Atoms are photo-excited by an X-ray interference field, formed during the (hkl) Bragg reflection from a substrate crystal. Traversing the Bragg reflection, the XSW intensity maxima move by half of the (hkl) diffraction plane spacing. The photoelectron signal from an adsorbate is accordingly modulated. The recorded signal is then fitted by a theoretical function, which yields two structural parameters called coherent fraction F and coherent position P, which are defined on a scale 0 to 1. These represent amplitude and phase, respectively, of the (hkl) Fourier component of the adsorbate distribution function. The parameter P can be translated into a distance $z_H = Pd_{hkl}$ with respect to the used reflection plane d_{hkl}, and the parameter F is a measure of the distribution around this position. For further details, the reader is referred to the literature.[33]

However, the reference frame for XSW measurements is the bulk unit cell of the used substrate crystal, here STO, and distances $z_H = Pd_H$ are determined relative to the bulklike, unrelaxed lattice/diffraction planes d_H, here d_{002} and d_{111}. When concluding on surface bond lengths, surface reconstruction/relaxation must be taken into account. With this in mind, the XSW result for atoms in the STO substrate can give an indication of the level of reconstruction present on the surface. The XSW analysis of the O 1s component corresponding to substrate O atoms, utilizing the (002) Bragg reflection for the as-prepared STO substrate, resulted in $P > 0$ and $F \ll 1$ across multiple different spots on the sample. In the ideal STO lattice, oxygen and Ti reside exactly on the

DOI: 10.1021/acs.jpcc.9b01730
J. Phys. Chem. C XXXX, XXX, XXX−XXX

Table 1. Summary of XSW Results[a]

		O (STO)		O(H)				$(H_2)O$		
Fig. (*hkl*)	*T* (K)	*F*	*P*	$\Theta_S\Theta_E$ (ML)	τ (min)	*F*	*P* [z_{001c}/Å]	$\Theta_S\Theta_E$ (ML)	*F*	*P* [z_{001c}/Å]
1c, 2a (111)	200	0.91	−0.04	1	40	0.28 ± 0.10	0.15 ± 0.12 [0.75 ± 0.5]	0.5	0.45 ± 0.04	0.11 ± 0.04
				0.6				0.1		[0.59 ± 0.2]
2b (002)	200	0.81	0.09	0.7	180	0.53 ± 0.05	0.15 ± 0.04 [0.12 ± 0.08]	0.7	0.43 ± 0.04	0.41 ± 0.04
				0.6				0.2		[0.62 ± 0.08]
1d, 2c (002)	200	0.58	0.06	0.3	5	0.40 ± 0.04	0.09 ± 0.05 [0.06 ± 0.1]	0.1	N/A	N/A
				0.2				0		
2d (002)	200	0.59	0.06	0.25	N/A	0.89 ± 0.03	0.06 ± 0.03 [0.00 ± 0.06]	0	N/A	N/A
				0.25						
2e (002)	300	0.72	0.01	0.25	1	0.74 ± 0.03	−0.04 ± 0.03	0	N/A	N/A
				0.25			[−0.10 ± 0.06]			

[a] *T* is the sample temperature. The coverages Θ_S and Θ_E refer to start and end, respectively, of the XSW scan. τ is an estimate of the half-life of the unstable OH on the surface. The [001] projected surface distance $z_{001c} = P_c d_H$ with the diffraction plane spacing H takes into account surface relaxation in a first approximation via $P_c = P - P_{O(STO)}$, where P is the measured position of OH or H_2O shown in Figure 2a–e (see the text and Supporting Information for more details).

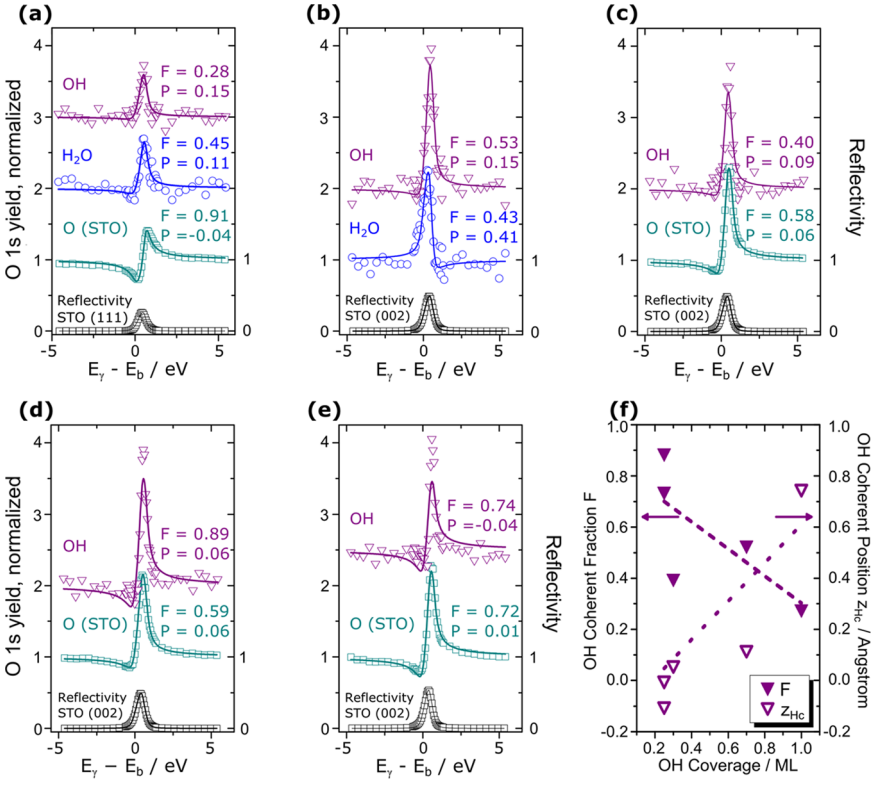

Figure 2. (a–e) XSW scans plotted vs. excitation energy around the Bragg energy E_b. Symbols are data, corrected for desorption, and lines are fits to the data. Starting coverages decrease from (a) to (e). (a) XSW scan of (111) reflection around 2.76 keV, (b) to (e) (002) reflections around 3.18 keV. (f) XSW results in terms of coherent fraction and distance $z_{Hc} = z_{001c}$, plotted as a function of OH coverage; lines are only meant to guide the eye. For more details see Table 1.

(002) planes, i.e., at $P = 0$. Thus, the XSW results for the STO oxygen indicate outward relaxation of surface oxygen. Both coherent position *P* and coherent fraction *F* of oxygen showed some variations when probing different spots on the surface (see Table 1). The XSW findings are thus in agreement with the LEED images, revealing an inhomogeneous, at least partially reconstructed, surface.

RESULTS

Figure 1b shows a photoelectron spectrum of the O 1s region recorded after water deposition. The O 1s peak has an asymmetric shape with a prolonged shoulder extending almost 5 eV beyond the main peak. Two components are clearly resolved and a third one by peak fitting. The largest one, at a binding energy of E_B = 530.8 eV, originates from the oxygen atoms in the bulk of STO. The other two components at E_B = 534.3 eV and E_B = 532.7 eV are attributed to the oxygen belonging to water and OH, respectively.[35] Obviously, a significant amount of the deposited water has dissociated. In Figure 1c,d we show the results of corresponding XSW scans, using the STO(111) reflection. With the O 1s yields of OH and H_2O plotted as a function of scan time, the figure shows

DOI: 10.1021/acs.jpcc.9b01730
J. Phys. Chem. C XXXX, XXX, XXX−XXX

that the O 1s signals and, thus, the coverages of both OH and H_2O decrease during the XSW measurement. For Figure 1c, 1 ML OH and 0.5 ML H_2O cover the surface at the beginning, of which 40 and 80%, respectively, desorb during the XSW scan. Fitting an exponential to the time dependence of the data reveals that H_2O tends to desorb completely, whereas 30%, i.e., about 1/4 ML of OH, appear to be stable on the surface (see Figure 1d). To evaluate the XSW data by standard analysis,[33,36] we removed the time-dependent part of the signal (see the Supporting Information for more details).

Fitting the accordingly generated XSW data, as shown in Figure 2a, provides the two dimensionless structural parameters, coherent fraction F and coherent position P.[33,36]

Converting the coherent position P to distance,[36] the oxygen atom of H_2O is located at $z_H = Pd_H + nd_H$. The position is only defined modulo n times the diffraction plane spacing d_H because of the periodicity of the standing wave. Setting n = 1, the distance projected onto the [001] direction becomes z_{001} = 0.43 + 1.95 Å = 2.38 Å above the TiO_2 diffraction plane (see the Supporting Information for details). We discard the shorter distance of 0.43 Å, since it corresponds to an unreasonably short bond length for the water molecule. For the hydroxyls, P = 0.15 corresponds to z_{001} = 0.59 Å or z_{001} = 2.54 Å above the TiO_2 diffraction plane. For determining surface distances from these values, which represent distance with respect to a bulklike surface plane, surface relaxations must be taken into account.

XSW results for the oxygen positions (see Figure 2 and Table 1) of the STO with $P \neq 0$ indicate that the Ti-oxide surface is not in the bulklike position, i.e., it does not coincide with the TiO_2 diffraction plane but is outward ($P > 0$) or inward ($P < 0$) relaxed (see the Supporting Information for more details). Inward relaxation of oxygen (and Ti) by less than a tenth of an Ångström, as found for the spot investigated by the (111) measurement, is expected for an unreconstructed surface.[37,31] Outward relaxation appears to be the result of surface reconstruction[38] (see further below). Taking surface relaxation due to reconstruction into account with the help of the STO oxygen signal, we calculate (in first approximation) surface distances for the oxygen of hydroxyls/water by $z_{Hc} = P_c d_H + nd_H$ using $P_c = P_{OH/H2O} - P_{O(STO)}$, with $P_{OH/H2O}$ and $P_{O(STO)}$ being the measured coherent positions of OH/H_2O and STO oxygen, respectively. Table 1 (first row) lists P-values and surface distances (z_{001c}) calculated in this way. This locates water at 0.59 ± 0.2 Å + 1.95 Å = 2.54 ± 0.2 Å and hydroxyl at 0.75 ± 0.5 Å or 0.75 + 1.95 = 2.70 ± 0.5 Å above the Ti-oxide surface.

The result of the XSW measurement using STO(002) reflection and a different spot on the surface, after necessary correction for desorption, is shown in Figure 2b. Fit to the XSW data (cf. Figure 2b and Table 1) shows for the oxygen atoms of OH and H_2O positions of 0.29 Å (P = 0.15) and 0.80 Å (P = 0.41), respectively, above the (002) diffraction plane (either SrO or TiO_2). Again taking outward relaxation of the surface into account (STO oxygen position P = 0.09 or Δz_{001} = 0.18 Å, cf. Table 1), this places the oxygen atom of H_2O at 2.57 ± 0.08 Å and OH at 0.12 ± 0.08 Å or 2.07 ± 0.08 Å above the Ti-oxide surface, respectively. We first concentrate on the result for H_2O and will come back to Figure 2c–e and the results for the OH further below.

The (111) and (002) results for the water-oxygen position are shown schematically in Figure 3 with respect to the STO bulk unit cell (in (110) orientation, cf. Figure 3a), which

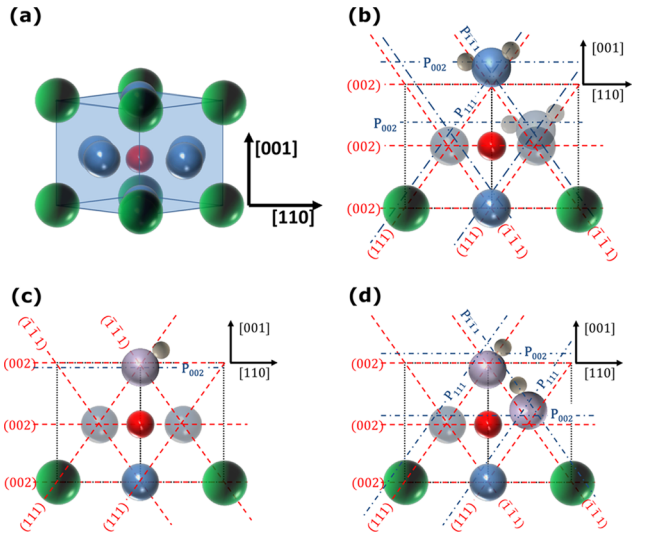

Figure 3. (a) STO unit cell in the (110) orientation with Ti in the center, oxygen at the face centers, and Sr at the corners. (b, c) Schematic representation of XSW results for OH and H_2O with respect to the STO bulk unit cell. In reality, the surface was found to be reconstructed. (b) XSW(111) and (002) results P_{111} and P_{002}, respectively, for the location of water on the TiO_2-terminated STO(001) surface are indicated as blue (dashed–dotted) lines. The (002) and (111) diffraction planes are indicated (red dashed lines). The water-oxygen is located close to the Ti atop site, i.e., the bulk oxygen position. (c) Graphical representation of the (002) result for the stable hydroxyl located 1.85 Å above the TiO_2 surface, probably atop Ti. (d) Graphical representation of the (111) and (002) result for the unstable hydroxyls, assuming two hydroxyls, i.e., an adsorbed hydroxyl and a hydroxylated oxygen surface atom (see the text for more details).

determines the XSW periodicity (cf. Figure 1a) and represents thus the reference for the XSW coherent position P. A corresponding image of the water-oxygen position created by Fourier back-transformation of the XSW data[39−41] is shown in the Supporting Information. Combining and averaging the results of the (111) and (002) measurements, the estimated surface distance of water becomes 2.56 ± 0.2 Å. This is significantly higher than those predicted by Guhl et al.[27] (2.21 Å), Evarestov et al.[26] (2.26 Å), and Hinojosa et al.[28] (2.27 Å) but, within error bar, somewhat in better agreement with the SXRD results of Hussain et al. In contact with bulk water, they located the oxygen atom of H_2O at 2.30 Å above the TiO_2 surface. In agreement with the above cited studies, our result suggests that the oxygen of the water molecule is located close to atop of a Ti surface atom (see Figure 3b). The (111) coherent fraction F = 0.45 indicates a wide distribution (≈0.5 Å rms) of water around the atop position that is in line with a water molecule tilted from the symmetry site[27,28] and its "free liberation".[26]

Figure 1b–d show that a major fraction of H_2O immediately deprotonates and that the remainder desorbs. Focusing now on the produced hydroxyl, Figure 1d shows the desorption of H_2O and OH during an (002) XSW scan with a lower coverage of 0.3 ML OH and 0.1 ML H_2O on the surface at the beginning of the XSW scan. The H_2O signal has vanished completely after about 12 min. Of the OH, 40% desorb with a time constant of about 1 min, but the measurement shows that 60% (about 0.2 ML) OH appear to be stable on the surface. Corrected for desorption, the result of the corresponding

DOI: 10.1021/acs.jpcc.9b01730
J. Phys. Chem. C XXXX, XXX, XXX−XXX

XSW(002) scan for OH is shown in Figure 2c. The corresponding values of F and P are listed in Table 1, and z_{Hc} takes into account surface relaxation using the O (STO) position (P = 0.06) in a first approximation for the amount of relaxation.

A tightly bound hydroxyl remains on the surface after water and the produced volatile hydroxyls have desorbed. Figure 2d shows the result of an XSW measurement started when the surface was already water-free. The OH coverage of 0.25 ML did not change during the scan, and the XSW result shows a very high coherent fraction (F = 0.89), indicating a well-defined adsorption site (surface distance) of this hydroxyl.

This remaining 1/4 ML OH is also stable at room temperature. This is shown in the O 1s XPS recorded at room temperature (inset of Figure 1b), where the O 1s peak from the STO shows a shoulder at E_B = 532.7 eV characteristic of 0.25 ML OH present on the surface. The XSW analysis (Figure 2e) yielded a high coherent fraction F = 0.74 for the hydroxyl, about the same value as for the bulk oxygen, indicative of a well-defined adsorption site. According to the XSW data, the Ti-oxide surface (STO oxygen P = 0.01) is almost in the bulk position. Using this estimate of a minor surface relaxation of +0.02 Å, the hydroxyl is located 1.85 ± 0.06 Å above the TiO_2 plane, as shown schematically in Figure 3c.

DISCUSSION

The surface position of the oxygen of the stable OH determined by XSW is in excellent agreement with distances calculated by Evarestov et al.[26] (1.88 Å), Guhl et al.[27] (1.84 Å), and Hinojosa et al.[28] (1.84 Å). The latter two density functional theory studies concluded that dissociative adsorption should occur on the TiO_2-terminated surface at low water coverages. Wang et al.[19] reported dissociative desorption features of water on Ti-oxide-terminated STO(001) in the temperature range 300−500 K. Beccera-Toledo et al.[23,29] suggested that dissociatively adsorbed water is essential for the formation of STO(001) reconstructions, such as the 2 × 1 and $c(4 \times 4)$. Using the coordinates for OH on the 2 × 1 surface, available in the Supporting Information of the above papers, the oxygen atoms of a monolayer of OH would be located at two positions for the (002) reflection: P = −0.076, and P = 0.0884, which results in an average position P = 0.01 and a coherent fraction F = 0.87. This is in reasonable agreement with the results of the measurement shown in Figure 2d (P = 0.06 and F = 0.89) for stable hydroxyls on an obviously reconstructed surface (oxygen of STO at P = 0.06). However, we find only 0.25 ML OH on the surface in contrast to the full ML in the calculation of Beccera-Toledo et al.

The most interesting finding of the present study is the immediate deprotonation of a large fraction (≈50%) of a monolayer of water already at 200 K. The produced hydroxyls are volatile, accompanying the desorbing water (cf. Figures 1c,d). The XSW data clearly distinguish the volatile from the 1/4 ML tightly bound hydroxyls. The small coherent fractions observed at higher OH coverages are indicative of OH, now occupying multiple sites. Plotting the XSW results as a function of OH coverages (cf. Figure 2f) shows that the mean distance of the hydroxyls from the surface increases with increasing OH coverage, whereas the coherent fraction F decreases. This is a clear indication that for coverages exceeding 0.25 ML, volatile hydroxyls, located at different positions from the stable OH, further increase the hydroxyl coverage. The XSW coherent position, representing a weighted mean position, shifts to a higher value accompanied by a decrease in the coherent fraction. Volatile OH are obviously located (on average) further from the (002) surface diffraction plane.

The volatile hydroxyls are an immediate product of the dissociation of the water molecule when it binds to the surface Ti atom. According to a widely accepted scenario,[26−28] upon adsorption of the water, one hydrogen is pulled toward a surface oxygen, leading to deprotonation of the water molecule. The liberated hydrogen attaches to a surface oxygen, which is lifted out of the surface[26−28] (by some 10th of an Å). The OH stays bound above titanium, now with a shorter bond length, roughly at the same position as the stable OH, though apparently less tightly bound. This scenario, in agreement with the XSW results, is represented schematically in Figures 3d and 4. The decomposition of one H_2O into two hydroxyls explains that the total coverage (OH plus H_2O) significantly exceeds 1 ML after dosing just 0.6 Langmuir H_2O (≈1 ML).

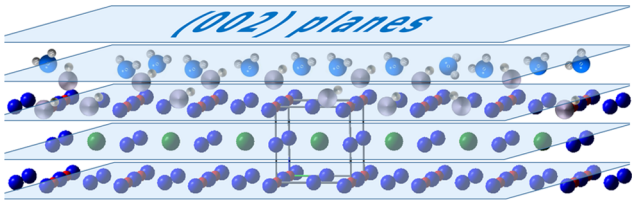

Figure 4. Schematic graphic representation of the result of the XSW/XPS measurement after deposition of about 1 ML H_2O, over-simplifyingly represented on a Ti-oxide-terminated, bulklike STO(001) surface. Water and OH supposedly adsorb above surface Ti, and about 0.5 ML of the Ti-oxide surface oxygen atoms are hydroxylated. The STO unit cell is indicated with Sr in the center. Color codes are as in Figures 1 and 3.

Only 0.25 ML OH atop Ti are stable and additional hydroxyls desorb together with H_2O. Table 1 lists estimated lifetimes of the volatile hydroxyls on the surface. The lifetime of the hydroxyls appears to be more than an order of magnitude longer in coexistence with H_2O. Water is obviously continuously deprotonated, in part replenishing the OH coverage, compensating for the loss due to desorption. Only when H_2O is consumed and/or has desorbed completely does the coverage of the hydroxyls decrease quickly, approaching 1/4 ML.

We can estimate the surface location of the volatile hydroxyls from the XSW measurements. The (111) and (002) results differ significantly, but for the former, the OH starting coverage (cf. Table 1) is higher and the coherent fraction is low, resulting in a larger error bar in the position. With a smaller OH coverage for the (002) measurement, the coherent fraction is higher (cf. Figure 2b and Table 1) and the position is lower. Nevertheless, to estimate the structure of the volatile hydroxyls, we combine both results (a corresponding Fourier transform image is shown in the Supporting Information), giving a mean position of the OH-oxygen of 0.23 ± 0.2 Å above the Ti-oxide surface plane. In fact, we can simulate this result by assuming two surface hydroxyls at two different positions, as shown in Figure 3d. The hydroxylated oxygen is lifted out of the surface by ≈0.4 Å, and the deprotonated OH remains bonded above Ti, just as the water molecule, but with a shorter Ti−O bond length of 1.85 Å, i.e, 0.1 Å below the Tioxide surface plane. This scenario with these two different hydroxyl surface sites leads to a mean surface

DOI: 10.1021/acs.jpcc.9b01730
J. Phys. Chem. C XXXX, XXX, XXX−XXX

distance of the OH-oxygen atoms of 0.15 Å and a (002) coherent fraction $F = 0.71$, in reasonable agreement with the (002) data ($z_{002c} = 0.12$ Å and $F = 0.53$). The measured (111) coherent fraction ($F = 0.28$) is much lower, indicating that the hydroxyls are displaced in-plane from the high-symmetry sites (see Figure S7).

Finally, we want to comment on the STO(001) surface. The results of the five XSW measurements listed in Table 1 show, in three cases, a significant outward shift ($P > 0$) of the STO oxygen, which can be assigned to reconstructed surface areas evidenced by the LEED measurements (see the Supporting Information). Because of a shallow mean electron escape angle of 15° for the (002) measurements, our photoelectron spectra are rather surface-sensitive. If we use coordinates for the $c(6 \times 2)$ surface provided in the Supporting Information of the paper of Ciston et al.,[38] we can calculate the (002) coherent position $P \approx 0.04$ for oxygen atoms and for titanium ($P \approx 0.1$) being even larger. This is qualitatively in agreement with our results.

CONCLUSIONS

In summary, we studied the adsorption and decomposition of water on a Ti-oxide-terminated STO(001) surface using photoelectron spectroscopy combined with the XSW technique. The XSW data of the inhomogeneous, in part $c(6 \times 2)$ reconstructed, STO(001) surface showed regions of significant outward relaxation of the surface layer in agreement with published data.[38] The surface is hydroxylated, even without previous exposure to water, which may be relevant for the formation or stabilization of Ti-oxide STO(001) surface structure/reconstructions.[23,29] At 200 K, a monolayer of water adsorbs with the oxygen of the water molecule at a position of 2.56 ± 0.2 Å roughly above Ti on the Ti-oxide surface, but the water molecule is unstable and ≈50% H_2O deprotonate immediately. Our XSW results suggest that the produced hydroxyls occupy positions atop surface titanium and the liberated hydrogen attaches to oxygen surface atoms. The majority of hydroxyls vanishes rapidly with the water. Whether the OH and H recombine and desorb as water remains an open question. It is found that 0.25 ML tightly bound hydroxyl remain on the surface, (most likely) above surface Ti, and are stable at room temperature. Because of desorption and surface reconstruction, the XSW structural data and determined bond lengths are associated with unusually large error bars. Nevertheless, we could clearly distinguish the volatile hydroxyls and provide some clues regarding their formation and structure. Their rapid formation at 200 K demonstrates that Ti-oxide-terminated STO(001) possesses a surprisingly high activity toward the deprotonation of water.

ASSOCIATED CONTENT

Supporting Information

The Supporting Information is available free of charge on the ACS Publications website at DOI: 10.1021/acs.jpcc.9b01730.

It provides experimental details and specifics of the XSW analysis (PDF)

AUTHOR INFORMATION

Corresponding Author

*E-mail: jorg.zegenhagen@diamond.ac.uk.

ORCID

David A. Duncan: 0000-0002-0827-2022

Pardeep K. Thakur: 0000-0002-9599-0531

Jörg Zegenhagen: 0000-0003-0752-5320

Notes

The authors declare no competing financial interest.

ACKNOWLEDGMENTS

We gratefully acknowledge time at the Diamond beamline I09 (proposal number SI-15132) and skillful assistance by Tien-Lin Lee and Dave McCue. Axel Wilson has received funding from the European Union's Horizon 2020 research and innovation program under the Marie Skłodowska-Curie grant agreement (GA) No 665593 awarded to the Science and Technology Facilities Council. Vladyslav Solokha acknowledges financial support by the Austrian Academy of Sciences via a DOC fellowship.

REFERENCES

(1) Fujishima, A.; Honda, K. Electrochemical photolysis of water at a semiconductor electrode. *Nature* **1972**, *238*, 37−38.

(2) Mavroides, J. G.; Kafalas, J. A.; Kolesar, D. F. Photoelectrolysis of water in cells with $SrTiO_3$ anodes. *Appl. Phys. Lett.* **1976**, *28*, 241−243.

(3) Wagner, F. T.; Ferrer, S.; Somorjai, G. A. Photocatalytic hydrogen production from water over $SrTiO_3$ crystal surfaces, electron spectroscopy studies of adsorbed H_2, O_2 and H_2O. *Surf. Sci.* **1980**, *101*, 462−474.

(4) de Kreuk, C. W.; de Groot, J. L. B.; Mackor, A. Photocorrosion of strontium titanate photoanodes. *Sol. Energy Mater.* **1981**, *5*, 437−444.

(5) Lv, M.; Xie, Y.; Wang, Y.; Sun, X.; Wu, F.; Chen, H.; Wang, S.; Shen, C.; Chen, Z.; Ni, S.; et al. Bismuth and chromium co-doped strontium titanates and their photocatalytic properties under visible light irradiation. *Phys. Chem. Chem. Phys.* **2015**, *17*, 26320−26329.

(6) Ohtomo, A.; Hwang, H. Y. A high-mobility electron gas at the $LaAlO_3/SrTiO_3$ heterointerface. *Nature* **2004**, *427*, 423−426.

(7) Brinkman, A. Streaks of conduction. *Nat. Mater.* **2013**, *12*, 1085−1086.

(8) Blank, D. H. A.; Rijnders, G. Oxides offer the write stuff. *Nat. Nanotechnol.* **2009**, *4*, 279−280.

(9) Schooley, J. F.; Hosler, W. R.; Cohen, M. L. Superconductivity in semiconducting $SrTiO_3$. *Phys. Rev. Lett.* **1964**, *12*, 474−475.

(10) Jiang, Q. D.; Zegenhagen, J. c(6 × 2) and c(4 × 2) reconstruction of $SrTiO_3$(001). *Surf. Sci.* **1999**, *425*, 343−354.

(11) Lanier, C. H.; van de Walle, A.; Erdman, N.; Landree, E.; Warschkow, O.; Kazimirov, A.; Poeppelmeier, K. R.; Zegenhagen, J.; Asta, M.; Marks, L. D. Atomic scale structure of the $SrTiO_3$(001)-c(6 × 2) reconstruction: experiments and first-principles calculations. *Phys. Rev. B: Condens. Matter Mater. Phys.* **2007**, *76*, No. 045421.

(12) Henrich, V. E.; Dresselhaus, G.; Zeiger, H. J. Chemisorbed phases of H_2O on TiO_2 and $SrTiO_3$. *Solid State Commun.* **1977**, *24*, 623−626.

(13) Webb, C.; Lichtensteiger, M. UPS/XPS study of reactive and non-reactive $SrTiO_3$(100) surfaces: adsorption of H_2O. *Surf. Sci. Lett.* **1981**, *107*, L345−L349.

(14) Egdell, R. G.; Naylor, P. D. The adsorption of water on $SrTiO_3$(100): a study of electron energy loss and photoelectron spectroscopies. *Chem. Phys. Lett.* **1982**, *91*, 200−205.

(15) Cox, P. A.; Egdell, R. G.; Naylor, P. D. HREELS studies of adsorbates on polar solids: water on $SrTiO_3$(100). *J. Electron Spectrosc. Relat. Phenom.* **1983**, *29*, 247−252.

(16) Brookes, N. B.; Thornton, G.; Quinn, F. M. $SrTiO_3$(100) step sites as catalytic centers for H_2O dissociation. *Solid State Commun.* **1987**, *64*, 383−386.

(17) Brookes, N. B.; Quinn, F. M.; Thornton, G. The involvement of step and terrace sites in H_2O adsorption on $SrTiO_3$(100). *Phys. Scr.* **1987**, *36*, 711−714.

DOI: 10.1021/acs.jpcc.9b01730
J. Phys. Chem. C XXXX, XXX, XXX−XXX

(18) Eriksen, S.; Naylor, P. D.; Egdell, R. G. The adsorption of water on $SrTiO_3$ and TiO_2: a reappraisal. *Spectrochim. Acta, Part A* **1987**, *43*, 1535−1538.
(19) Wang, L.-Q.; Ferris, K. F.; Herman, G. S. Interactions of H_2O with $SrTiO_3$(100) surfaces. *J. Vac. Sci. Technol., A* **2002**, *20*, 239−244.
(20) Iwahori, K.; Watanabe, S.; Kawai, M.; et al. Effect of water adsorption on microscopic friction force on $SrTiO_3$(001). *J. Appl. Phys.* **2003**, *93*, 3223−3227.
(21) Kato, H. S.; Shiraki, S.; Nantoh, M.; Kawai, M. Water reaction on $SrTiO_3$(001): promotion effect due to condensation. *Surf. Sci.* **2003**, *544*, L722−L728.
(22) Baniecki, J. D.; Ishii, M.; Kurihara, K.; Yamanaka, K.; Yano, T.; Shinozaki, K.; Imada, T.; Kobayashi, Y. Chemisorption of water and carbon dioxide on nanostructured surfaces. *J. Appl. Phys.* **2009**, *106*, No. 054109.
(23) Becerra-Toledo, A. E.; Castell, M. R.; Marks, L. D. Water adsorption on $SrTiO_3$(001): I. Experimental and simulated STM. *Surf. Sci.* **2012**, *606*, 762−765.
(24) Hussain, H.; Torrelles, X.; Rajput, P.; Nicotra, M.; Thornton, G.; Zegenhagen, J. A quantitative structural investigation of the 0.1 wt % Nb− $SrTiO_3$(001)/H_2O interface. *J. Phys. Chem. C* **2014**, *118*, 10980−10988.
(25) Kawasaki, S.; Holmström, E.; Takahashi, R.; Spijker, P.; Foster, A. S.; Onishi; Lippmaa, M. Intrinsic superhydrophilicity of titania-terminated surfaces. *J. Phys. Chem. C* **2017**, *121*, 2268−2275.
(26) Evarestov, R. A.; Bandura, A. V.; Alexandrov, V. E. Adsorption of water on (001) surface of $SrTiO_3$ and $SrZrO_3$ cubic perovskites: hybrid HF-DFT LCAO calculations. *Surf. Sci.* **2007**, *601*, 1844−1856.
(27) Guhl, H.; Miller, W.; Reuter, K. Water adsorption and dissociation on $SrTiO_3$(001) revisited: a density functional theory study. *Phys. Rev. B* **2010**, *81*, No. 155455.
(28) Hinojosa, B. B.; Cleve, T. V.; Asthagiri, A. A first-principles study of H_2O adsorption and dissociation on the $SrTiO_3$(100) surface. *Mol. Simul.* **2010**, *36*, 604−617.
(29) Becerra-Toledo, A. E.; Enterkin, J. A.; Kienzle, D. M.; Marks, L. D. Water adsorption on $SrTiO_3$(001): II. Water, water, everywhere. *Surf. Sci.* **2012**, *606*, 791−802.
(30) Martirez, J. M. P.; Kim, S.; Morales, E. H.; Diroll, B. T.; Cargnello, M.; Gordon, T. R.; Murray, C. B.; Bonnell, D. A.; Rappe, A. M. Synergistic oxygen evolving activity of a TiO_2-rich reconstructed $SrTiO_3$(001) surface. *J. Am. Chem. Soc.* **2015**, *137*, 2939−2947.
(31) Holmström, E.; Spijker, P.; Foster, A. S. The interface of $SrTiO_3$ and H_2O from density functional theory molecular dynamics. *Proc. R. Soc. A* **2016**, *472*, No. 20160293.
(32) Batterman, B. W. Effect of dynamical diffraction in x-ray fluorescence scattering. *Phys. Rev.* **1964**, *133*, A759−A764.
(33) Zegenhagen, J. Surface structure determination with X-ray standing waves. *Surf. Sci. Rep.* **1993**, *18*, 202−271.
(34) Lee, T.-L.; Duncan, D. A. A Two-color beamline for electron spectroscopies at Diamond Light Source. *Synchrotron Radiat. News* **2018**, *31*, 16−22.
(35) Li, W.; Liu, S.; Wang, S.; Guo, Q.; Guo, J. The roles of reduced Ti cations and oxygen vacancies in water adsorption and dissociation on $SrTiO_3$(110). *J. Phys. Chem. C* **2014**, *118*, 2469−2474.
(36) Zegenhagen, J. Surface Structure Analysis with X-ray Standing Waves. *Surface Science Techniques*; Bracco, G.; Holst, B., Eds.; Springer Series in Surface Science; Springer-Verlag: Berlin, 2013; pp 249−275.
(37) Eglitis, R. I.; Vanderbilt, D. First-principles calculations of atomic and electronic structure of $SrTiO_3$ (001) and (011) surfaces. *Phys. Rev. B* **2008**, *77*, No. 195408.
(38) Ciston, J.; Brown, H. G.; D'Alfonso, A. J.; Koirala, P.; Ophus, C.; Lin, Y.; Suzuki, Y.; Inada, H.; Zhu, Y.; Allen, L. J.; et al. Surface determination through atomically resolved secondary-electron imaging. *Nat. Commun.* **2015**, *6*, No. 7358.
(39) Hertel, N.; Materlik, G.; Zegenhagen, J. X-ray standing wave analysis of bismuth implanted in Si(110). *Z. Phys. B: Condens. Matter* **1985**, *58*, 199−204.
(40) Zhang, Z.; Fenter, P.; Cheng, L.; Sturchio, N. C.; Bedzyk, M. J.; Machesky, M. L.; Wesolowski, D. J. Model-independent x-ray imaging of adsorbed cations at the crystal−water interface. *Surf. Sci.* **2004**, *554*, L95−L100.
(41) Lee, T.-L.; Bihler, C.; Schoch, W.; Limmer, W.; Daeubler, J.; Thiess, S.; Zegenhagen, J.; et al. Fourier transform imaging of impurities in the unit cells of crystals: Mn in GaAs. *Phys. Rev. B.* **2010**, *81*, No. 235202.

DOI: 10.1021/acs.jpcc.9b01730
J. Phys. Chem. C XXXX, XXX, XXX−XXX